

\*Work supported in part by the National Science Foundation.

†Present address: Rockefeller Foundation, New York, New York.

<sup>1</sup>K. W. Jones, A. Z. Schwarzschild, E. K. Warburton, and D. B. Fossan, *Phys. Rev.* **178**, 1773 (1969).

<sup>2</sup>S. H. Henson, S. Cochavi, M. Marmor, and D. B. Fossan, *Phys. Rev. C* **3**, 191 (1971).

<sup>3</sup>K. A. Snover, J. M. McDonald, D. B. Fossan, and E. K. Warburton, *Phys. Rev. C* **4**, 398 (1971).

<sup>4</sup>O. Häusser, T. K. Alexander, and C. Broude, *Can. J. Phys.* **46**, 1035 (1968).

<sup>5</sup>G. A. Bissinger, P. A. Quin, and P. R. Chagnon, *Nucl.*

*Phys.* **A132**, 529 (1969).

<sup>6</sup>M. Marmor, S. Cochavi, S. H. Henson, and D. B. Fossan, *Bull. Am. Phys. Soc.* **14**, 628 (1969).

<sup>7</sup>J. L. Durell, P. R. Alderson, D. C. Bailey, L. L. Green, M. W. Greene, A. N. James, and J. F. Sharpey-Schafer, *J. Phys.* **A5**, 302 (1972). The errors quoted by these authors do not include any uncertainty for the stopping power.

<sup>8</sup>D. A. Hutcheon, W. C. Olsen, D. H. Sykes, and C. W. Vernetto, to be published.

<sup>9</sup>P. Wasielewski and F. B. Malik, *Nucl. Phys.* **A160**, 113 (1971).

<sup>10</sup>G. Morpurgo, *Phys. Rev.* **110**, 721 (1958).

PHYSICAL REVIEW C

VOLUME 6, NUMBER 6

DECEMBER 1972

## <sup>12</sup>C(<sup>16</sup>O, α)<sup>24</sup>Mg Excitation Functions and Statistical-Model Calculations for High-Spin States in <sup>24</sup>Mg<sup>†</sup>

L. R. Greenwood, K. Katori, R. E. Malmin, T. H. Braid, J. C. Stoltzfus, and R. H. Siemssen

*Argonne National Laboratory, Argonne, Illinois 60439*

(Received 17 July 1972)

High-resolution excitation functions were measured in the energy range  $E_{c.m.} = 19\text{--}25$  MeV for the <sup>12</sup>C(<sup>16</sup>O, α) reaction to highly excited states in <sup>24</sup>Mg ( $E_{exc} \approx 13.5\text{--}17.5$  MeV). The strong, rapid observed fluctuations suggest a predominately compound-nucleus reaction mechanism. The selective population of high-spin states in <sup>24</sup>Mg by the present reaction in contrast to the lack of such selectivity in the <sup>14</sup>N(<sup>14</sup>N, α) reaction can readily be explained by Hauser-Feshbach statistical-model calculations. A fluctuation analysis indicates coherence widths of 90–150 keV, and cross correlations were found to be small and thus compatible with a purely statistical compound-nucleus process.

### I. INTRODUCTION

The selective population of prominent states at high excitation in <sup>24</sup>Mg, observed by Middleton, Garrett, and Fortune<sup>1</sup> in the <sup>16</sup>O(<sup>12</sup>C, α) reaction, as well as the absence of such selectivity in the <sup>14</sup>N(<sup>14</sup>N, α) reaction, has led to much interest and speculation concerning the nature of the reaction mechanism for populating these states.<sup>2–5</sup> With a direct-reaction mechanism (e.g., <sup>8</sup>Be transfer), the selective population of a few states in a region of many overlapping levels would be due to nuclear-structure or angular-momentum-matching effects. A semidirect mechanism proceeding through doorway states of quartet character, for example, might also explain the selectivity. Evidence for such processes has been found recently by Middleton *et al.*,<sup>6</sup> who studied the <sup>12</sup>C(<sup>12</sup>C, α)<sup>20</sup>Ne reaction in which two  $K = 0$  bands at very nearly the same excitation energy were observed to be populated with very different intensities.

Alternatively, as proposed in this paper, the selective population of states in <sup>24</sup>Mg may be explained by a compound-nucleus reaction mecha-

nism. For the largest angular momenta brought into the compound nucleus in a heavy-ion collision, there will be only a few open channels that can carry away the angular momentum, and therefore these channels will be strongly populated. As shown in more detail later, this leads to a selective population of high-spin states, regardless of their structure. Particle-particle correlations show that the prominent states in <sup>24</sup>Mg indeed have high spin.<sup>2,5</sup> We have performed Hauser-Feshbach statistical-model calculations which readily explain the salient features of the <sup>12</sup>C(<sup>16</sup>O, α)<sup>24</sup>Mg and the <sup>14</sup>N(<sup>14</sup>N, α)<sup>24</sup>Mg reactions. This compound-nucleus picture is also in accord with the earlier results of Halbert, Durham, and van der Woude,<sup>7</sup> who studied the <sup>12</sup>C(<sup>16</sup>O, α) reaction to the first few excited states in <sup>24</sup>Mg at lower incident energies. Similar statistical-model calculations for heavy-ion reactions have also been performed by Vogt *et al.*<sup>8</sup> for the <sup>12</sup>C(<sup>12</sup>C, α)<sup>20</sup>Ne reaction and by Shaw *et al.*<sup>9</sup> for the <sup>16</sup>O(<sup>16</sup>O, α)<sup>28</sup>Si reaction.

Supporting evidence for the compound-nucleus picture also arises from elastic scattering studies. Whereas compound elastic effects are

strong in the  $^{12}\text{C} + ^{16}\text{O}$  scattering,<sup>10</sup> as evidenced by large fluctuations, the  $^{14}\text{N} + ^{14}\text{N}$  excitation functions<sup>11</sup> are very smooth.

In order to investigate the reaction mechanism further, high-resolution excitation functions were measured for the  $^{12}\text{C}(^{16}\text{O}, \alpha)$  reaction over the energy range  $E_{\text{c.m.}} = 19\text{--}25$  MeV for excitation energies  $E_x = 13.5\text{--}17.5$  MeV in  $^{24}\text{Mg}$  by use of a recently developed position-sensitive proportional counter<sup>12</sup> in the focal plane of an Enge split-pole spectrograph. Preliminary accounts of the present work on the excitation-function measurements<sup>13</sup> and the statistical-model calculations<sup>14</sup> were presented in 1971 at the Saclay conference. Similar excitation-function measurements with poorer energy resolution were recently reported by Gastebois *et al.*,<sup>3</sup> Stokstad *et al.*,<sup>15</sup> and by Cosman *et al.*<sup>16</sup> Strong and rapid fluctuations observed in the present excitation functions support a compound-nucleus reaction mechanism. The data have been subjected to a fluctuation analysis and in addition Hauser-Feshbach calculations have been performed. Although a significant direct-reaction component cannot be excluded in the present analysis, the available data are in good agreement with the simple Hauser-Feshbach statistical compound-nucleus model.

## II. EXPERIMENTAL PROCEDURE

The excitation functions were measured with self-supporting carbon foils, about  $5 \mu\text{g}/\text{cm}^2$  and thus about 40 keV thick to the incident  $^{16}\text{O}$  beam from the Argonne FN tandem accelerator. In order to minimize carbon buildup on the targets, they were enclosed in a copper sleeve cooled by liquid air. The carbon buildup measured  $1 \mu\text{g}/\text{cm}^2$  per mC of beam particles, as compared with about 5 times this rate without the cold sleeve.

The  $\alpha$  particles emitted at an angle of  $7.5^\circ$  (lab) were momentum-analyzed by an Enge split-pole spectrograph with a solid angle of  $2 \times 10^{-3}$  sr and were detected in the focal plane by a recently developed wire proportional counter.<sup>12</sup> This combination made the experiment feasible, since we were able to obtain a large number of high-resolution spectra in a rather short time. Furthermore, the data were available for on-line analysis; it was not necessary to develop and scan hundreds of nuclear emulsions.

The counter measured 24 cm in active length, and its position resolution was about 1 mm [full width at half maximum (FWHM)]. The counter consisted of a single high-resistance wire enclosed in a sealed box filled with a mixture of argon (90%) and methane (10%) at a pressure of 1 atm. Particles enter the counter through aluminized Mylar windows. The particle position was determined by

using a time-to-amplitude converter (TAC) to measure the difference between the rise times of the pulses traveling towards the two ends of the anode wire, a procedure due to Borkowski and Kopp.<sup>17</sup> The anode pulses were also summed to obtain a signal proportional to the energy loss  $\Delta E$ . The  $\Delta E$  signal was then used to discriminate against unwanted particles or noise by gating the TAC. The resultant TAC pulses were analyzed by an analog-to-digital converter, stored in the memory of an on-line ASI computer, and recorded on magnetic tape.

## III. RESULTS

The spectra, such as those shown in Fig. 1, were analyzed with the peak-fitting computer code AUTOFIT.<sup>18</sup> A composite spectrum obtained by taking five overlapping runs with the counter is shown in Fig. 2 for  $E_{\text{exc}} = 0\text{--}22$  MeV. The combination of

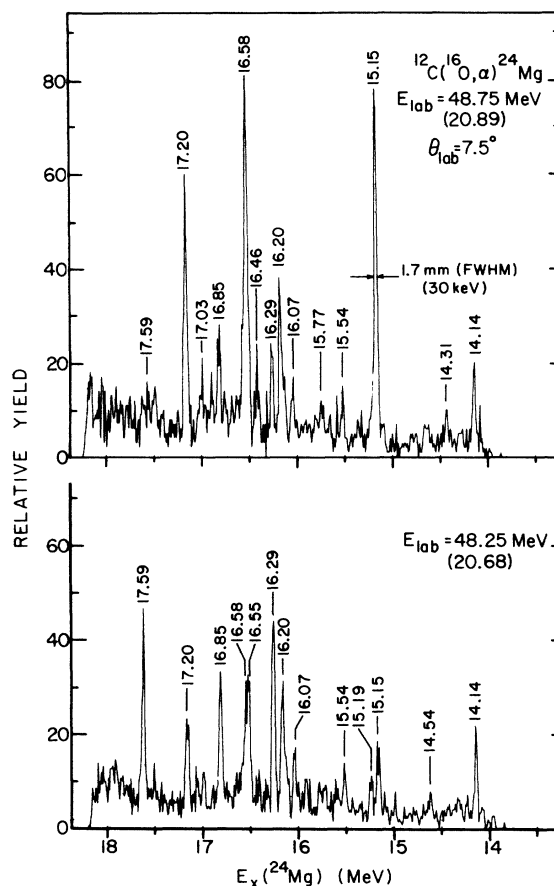


FIG. 1. Comparison between sample spectra for  $E_{\text{lab}} = 48.75$  and  $48.25$  MeV. Note the strong and rapid changes in the prominent states. The resolution in this case was about 30 keV (FWHM), although most of the data were taken with poorer resolution ( $\sim 50$  keV FWHM).

a large continuous background (due to low-spin states and breakup) and the high density of rapidly fluctuating levels made it difficult to extract small yields (<0.5 mb/sr). Furthermore, some transitions were not adequately resolved; in particular, the 14.14- and 16.55-MeV yields include contributions from adjacent states. The 16.55- and 16.59-MeV yields were added together, since they were not always resolved. However, the 16.59-MeV ( $6^+$ ) state is strong below  $E_{c.m.} \approx 21$  MeV, but virtually disappears at higher energies. Ten levels were analyzed completely, five more were analyzed over parts of the energy range, and at least 10 more can be distinguished at selected energies. All of the levels seen are given in Table I. Absolute excitation energies were measured to within  $\pm 30$  keV and were normalized to previously reported values for convenience.

Absolute cross sections were determined by measuring the ratio of the  $\alpha$  yield to the elastic scattering intensity for all charge states. Elastic angular distributions were then measured and compared with optical-model calculations, which give nearly the same results as Rutherford scattering at small angles. Corrections for carbon buildup were determined by repeated measurements. The estimated error in the absolute cross sections is  $\pm 30\%$ . It should be noted that the preliminary

cross sections published previously<sup>13</sup> in the proceedings of the Saclay conference were found to be too large by a factor of 1.6. Further, as a result of a recent energy recalibration at the Argonne tandem accelerator, the energy scale has been changed by about 0.6%, i.e., by about 200 keV (c.m.) at 48 MeV.

Excitation functions for the 10 most prominent levels are shown in Figs. 3 and 4. The excitation functions are dominated by strong, rapid fluctuations over the entire energy range. Such fluctuations are typical of compound-nucleus formation and are in sharp contrast to previous results by Gastebois *et al.*,<sup>3</sup> but in agreement with the results of Stokstad *et al.*<sup>15</sup> There do not appear to be any significant cross correlations between the excitation functions, and this conclusion is supported by a fluctuation analysis (Sec. IV).

The total  $\alpha$  yield observed between  $E_{exc} = 13.5$  and 17.5 MeV was obtained by summing all counts in the spectrum from the proportional counter, after correcting for changes in the spectrograph dispersion. The result (Fig. 5) is a very smooth function of energy. Also shown is the sum of all 10 of the most prominent levels (Figs. 3 and 4) and the difference between this sum and the total yield. The sum we presume corresponds to all of the high-spin states ( $I \geq 6$ ) while the difference is the

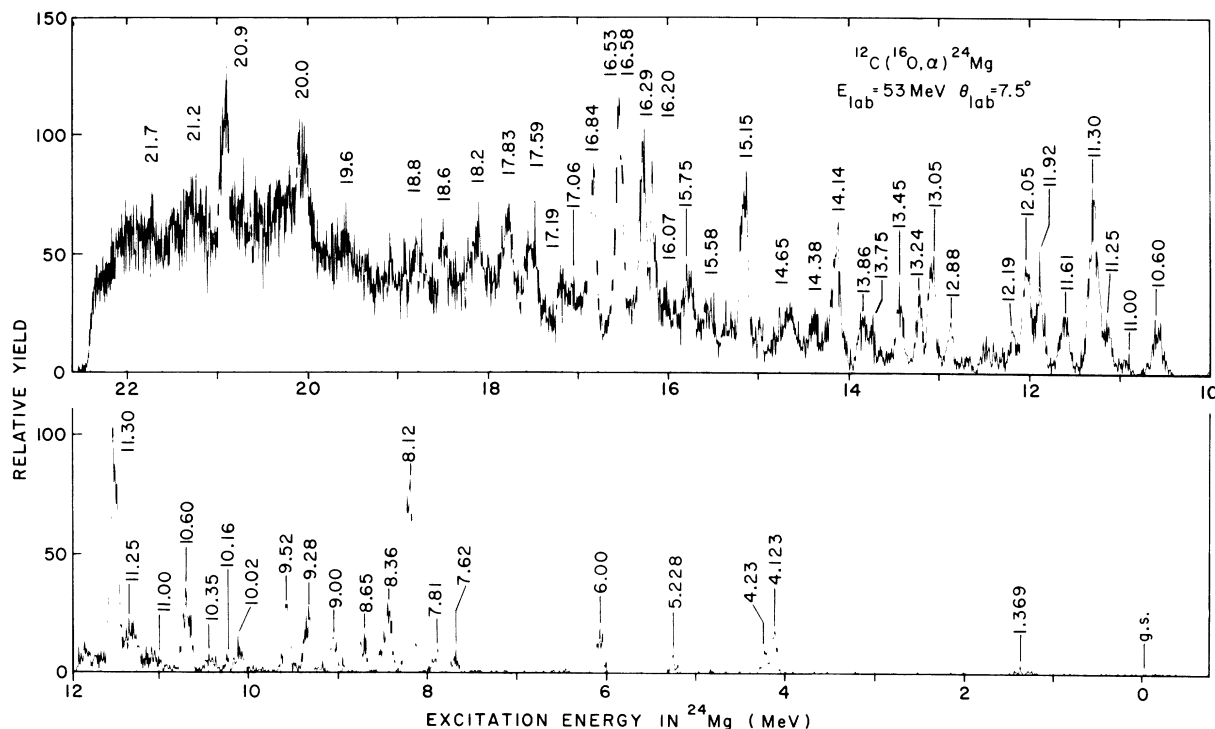


FIG. 2. A composite spectrum obtained by taking five overlapping counter spectra. The reaction at an incident energy of 53 MeV gives excitations up to  $E_x = 22$  MeV. The resolution at the highest excitation energies is poor because of an error in the computer code used to calculate kinematic-shift corrections.

sum of all low-spin states ( $I \leq 5$ ). The fact that all of these functions have a smooth energy dependence indicates that there are no large cross correlations and that the reaction is consistent with a purely statistical process. The solid lines are Hauser-Feshbach statistical-model calculations (Sec. V) which agree very well with the total yield and with the trend of the data.

The angular distributions of the total  $\alpha$  yield (Fig. 6) were also measured at three energies. Individual levels were not resolved due to an error in the computed kinematic corrections for the spectrograph. The dashed lines in the figure are least-squares fits to the function  $1/\sin\theta$ , which is the expected energy-averaged angular distribution for a statistical compound-nucleus model involving many large angular momenta.<sup>19</sup> Supporting evidence by Middleton *et al.*<sup>6</sup> has shown that energy-averaged angular distributions for states at lower

excitation ( $E_x = 5.22$ – $9.28$  MeV) indeed have very nearly a  $1/\sin\theta$  angular distribution.

#### IV. FLUCTUATION ANALYSIS

In order to determine to what degree the excitation functions are compatible with a purely compound-nucleus process, a standard Ericson<sup>20</sup> fluctuation analysis was performed for all levels. Autocorrelations were determined by use of the relation

$$R(\Gamma, \epsilon) = \frac{\langle \sigma(E)\sigma(E+\epsilon) \rangle}{\langle \sigma(E) \rangle \langle \sigma(E+\epsilon) \rangle} - 1,$$

where  $\sigma(E)$  is the measured differential cross section at energy  $E$ ,  $\epsilon$  is the energy interval, and  $\Gamma$

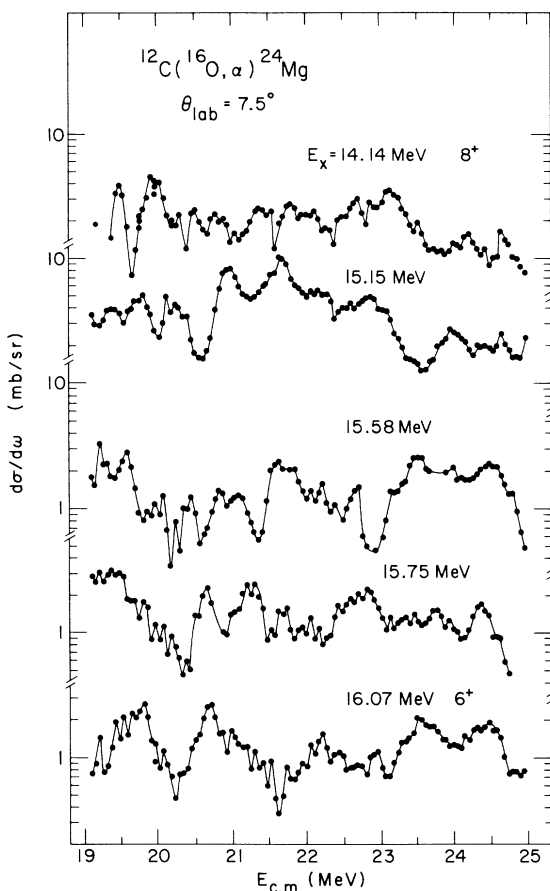


FIG. 3. Excitation functions for five prominent levels below 16.1 MeV in  $^{24}\text{Mg}$ . The incident energy was varied over the range  $E_{c.m.} = 19$ – $25$  MeV in steps of 54 keV (c.m.). Note that the functions are plotted on a logarithmic scale.

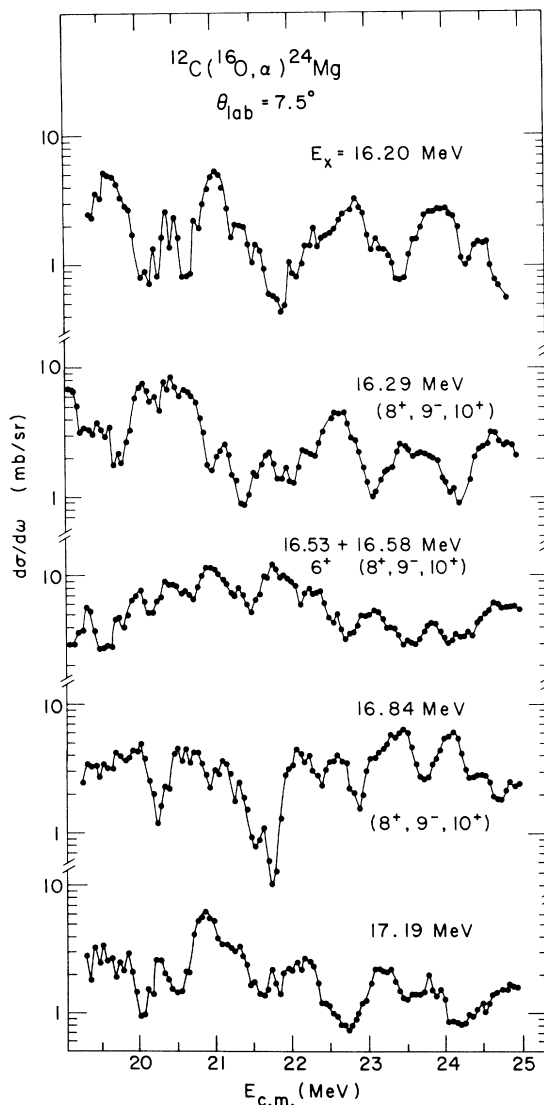


FIG. 4. Excitation functions for five prominent levels above 16.1 MeV in  $^{24}\text{Mg}$ .

is the average coherence width  $\langle \Gamma_I \rangle$ . Average cross sections were calculated by the method of moving averages, in which the averaging interval was varied to obtain consistency for  $R(\Gamma, 0)$  and  $\Gamma$ . The coherence width  $\Gamma$  was taken as the half-height on the assumption that  $R(\Gamma, \epsilon)$  has the Lorentzian shape

$$R(\Gamma, \epsilon) = \frac{\Gamma^2}{\Gamma^2 + \epsilon^2} \frac{[1 - Y_d^2]}{N_{\text{eff}}},$$

where  $N_{\text{eff}}$  is the number of effective open channels and  $Y_d$  is the ratio of the direct to the total cross section. The resulting values of  $R(\Gamma, 0)$  and  $\Gamma$  are given in Table I. The coherence widths varied from 90 to 150 keV, and the values of  $R(\Gamma, 0)$  varied from 0.05 to 0.22. If  $Y_d$  is small, the finite size of the statistical sample of data introduces about a 10–20% error in  $\Gamma$  and in  $R(\Gamma, 0)$ . The rather small values of  $R(\Gamma, 0)$  imply either a sizable direct-reaction component or large values of  $N_{\text{eff}}$ .

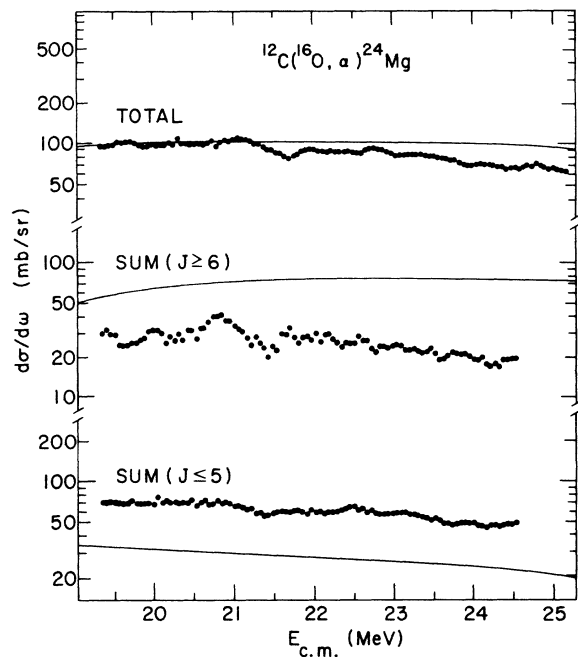


FIG. 5. Total  $\alpha$  yields for the excitation range  $E_x = 13.5$ – $17.5$  MeV in  $^{24}\text{Mg}$ . The top points are the total  $\alpha$  yield seen by the proportional counter. The middle points are the sums of the cross sections to the ten most prominent peaks (shown in Fig. 3 and 4). The bottom points represent the “background” obtained by subtracting the sum of the 10 most prominent peaks from the total. The smooth curves are Hauser-Feshbach calculations in which it was assumed that the sum of the 10 most prominent levels represent all high-spin states ( $I \geq 6$ ) and that the “background” was due to low-spin states ( $I \leq 5$ ). Note that the total yield is well described by the calculations.

In addition to the foregoing analysis, probability distributions for the ratio  $y = \sigma(E)/\langle \sigma(E) \rangle$  were computed in an attempt to obtain better limits on the values of  $Y_d$  and  $N_{\text{eff}}$ . These probability distributions are described by a modified  $\chi^2$  distribution.<sup>21</sup> If  $Y_d$  is assumed to be zero (no direct-reaction component), then  $N_{\text{eff}}$  must lie between 4 and 14, depending on the level in question. The number of open channels can have values in the range  $1 \leq N_{\text{eff}} \leq \frac{1}{2}(2I+1)$ , where  $I$  is the spin of the final state. It is expected to rise rapidly from  $N_{\text{eff}} = 1$  at  $0^\circ$  to  $\frac{1}{2}(2I+1)$  at  $90^\circ$ , the rapid increase with angle being due to the large angular momentum involved in the  $^{12}\text{C}(^{16}\text{O}, \alpha)^{24}\text{Mg}$  reaction. For the present case of  $\theta_{\text{c.m.}} = 12^\circ$ ,  $N_{\text{eff}}$  has been estimated<sup>22</sup> at about half the maximum value, which is  $N_{\text{eff}} = 4$ – $6$  for  $I = 6$ – $10$ . The fact that the measured values of  $N_{\text{eff}}$  are slightly larger than expected may be due to several factors. First of all, the value  $N_{\text{eff}} = 5$  implies that  $R(\Gamma, 0) \leq 0.2$ , the actual value depending on  $Y_d$ , and one might question the accuracy with which such a

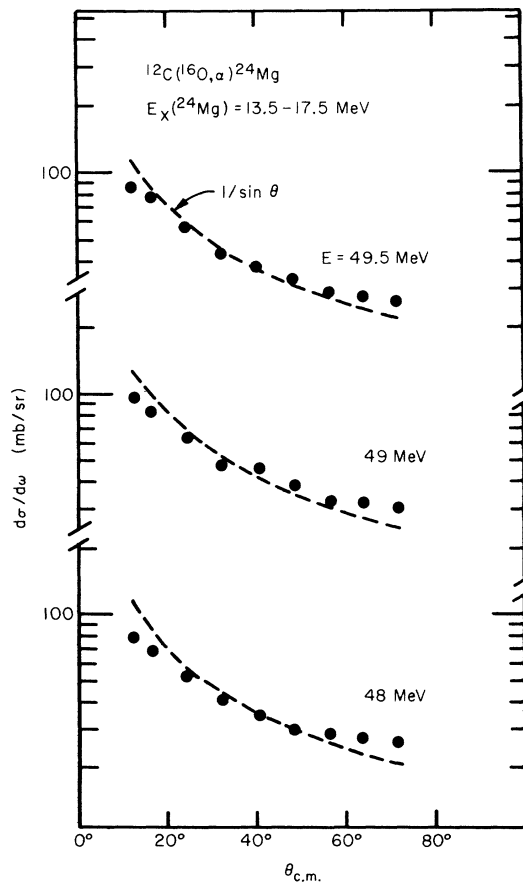


FIG. 6. Total  $\alpha$  angular distributions for  $E_x = 13.5$ – $17.5$  MeV in  $^{24}\text{Mg}$  for incident energies of 48, 49, and 49.5 MeV. The dashed lines are least-squares fits to the function  $1/\sin\theta$ .

small value of  $R(\Gamma, 0)$  can be determined. This is especially of concern, since many of the levels are not isolated but contain measurable contributions from nearby states. For example, the 14.14- and the 16.55–16.59-MeV levels were not resolved, and these showed the highest values of  $N_{\text{eff}}$ . Further, all of the levels ride on a continuous background due to low-spin states and breakup. As previously mentioned, the background subtraction was difficult for low yields ( $\leq 0.5$  mb/sr); and the resulting uncertainty might tend to fill in the minima in the excitation functions and thus lead to smaller values for  $R(\Gamma, 0)$  and, if  $Y_d \approx 0$ , to larger

required values of  $N_{\text{eff}}$ . The highest resolution used in the present experiment was 50 keV (FWHM), which was not sufficient to resolve many closely spaced weak levels observed at all excitation energies throughout the excitation function.

In order to ascertain whether or not the excitation functions showed significant correlations between transitions to different final states, cross correlations were computed from the relationship

$$R_\epsilon(\alpha, \alpha') = \frac{\langle \sigma_\alpha(E) \sigma_{\alpha'}(E + \epsilon) \rangle}{\langle \sigma_\alpha(E) \rangle \langle \sigma_{\alpha'}(E + \epsilon) \rangle} - 1$$

for the 10 excitation functions. The values were

TABLE I. Observed levels in  $^{24}\text{Mg}$ , with measured and calculated cross sections, autocorrelation coefficients  $R(\Gamma, 0)$ , and coherence widths from fluctuation analysis.

$E_x(^{24}\text{Mg})^a$ (MeV)	$\left\langle \frac{d\sigma}{d\Omega}(12^\circ) \right\rangle_{\text{exp}}^b$ (mb/sr)	$J^\pi$	$\left\langle \frac{d\sigma}{d\Omega}(12^\circ) \right\rangle_{\text{H.F.}}^c$ (mb/sr)	$R(\Gamma, 0)$	$\Gamma$ (keV)
13.86	1.2	5 <sup>-d</sup>	0.3	0.12	95
14.14	2.0	} 5 <sup>-d</sup> 8 <sup>+e</sup>	0.3	0.07	75
14.31	0.8 <sup>f</sup>		2.3		
14.54	1.1 <sup>f</sup>				
14.90	0.6 <sup>f</sup>				
15.15	3.8	} 4 <sup>+d</sup> (9 <sup>+</sup> ) <sup>g</sup>	0.06	0.08	110
15.19	1.5 <sup>f</sup>		1.8		
15.77	1.4			0.09	100
16.08	1.2	6 <sup>+h</sup>	0.3	0.14	120
16.22	1.9			0.22	145
16.29	3.0	} 8 <sup>+e</sup> 9 <sup>-e</sup> 10 <sup>+e</sup>	1.3	0.15	135
			1.8		
			4.4		
16.46	<1				
16.55	} 5.8 <sup>i</sup>	} 8 <sup>+e</sup> 9 <sup>-e</sup> 10 <sup>+e</sup> 6 <sup>+h</sup>	1.2	0.05	100
			1.7		
			4.1		
16.59			0.2		
	} 6 <sup>+d</sup> 8 <sup>+e</sup> 9 <sup>-e</sup> 10 <sup>+e</sup>	} 0.2 1.0 1.4 3.7		0.13	120
16.85			3.2		
16.93	<1 <sup>f</sup>				
17.03	<1 <sup>f</sup>				
17.20	2.0			0.125	125
17.52	<1 <sup>f</sup>				
17.59	<2 <sup>f</sup>				

<sup>a</sup> Absolute energies normalized to other work (Refs. 1 and 4). Accuracy in present work  $\pm 30$  keV.

<sup>b</sup> Present work. Energy-averaged from 19–25 MeV (c.m.).

<sup>c</sup> Hauser-Feshbach cross section at  $12^\circ$ , calculated on the assumption of a  $1/\sin\theta$  angular distribution.

<sup>d</sup> M. J. LeVine *et al.*, Bull. Am. Phys. Soc. **17**, 77 (1972).

<sup>e</sup> Reference 5.

<sup>f</sup> Not seen at all energies.

<sup>g</sup> Suggested by Ref. 4, although unlikely due to work of Ref. 2.

<sup>h</sup> Reference 2.

<sup>i</sup> The 16.55-MeV level (8<sup>+</sup>, 9<sup>-</sup>, 10<sup>+</sup>) was not resolved from the 16.59-MeV level (6<sup>+</sup>), although the 16.59-MeV level was weakly populated above  $E_{\text{c.m.}} \approx 21$  MeV.

TABLE II. Level-density parameters (Ref. a)  $a$ ,  $\Delta$ ,  $Y$ ,  $E_c$ , and  $E_{\max}$ , optical-model parameters  $V$ ,  $r_0$ ,  $a_0$ ,  $W$ ,  $r_i$ , and  $a_i$ , and the Coulomb interaction radius  $R_{\text{Coul}}$ .

	$^{24}\text{Mg} + \alpha$	$^{27}\text{Al} + p$	$^{27}\text{Si} + n$	$^{26}\text{Al} + d$	$^{25}\text{Mg} + ^3\text{He}$	$^{23}\text{Na} + ^5\text{Li}$	$^{20}\text{Ne} + ^8\text{Be}$	$^{14}\text{N} + ^{14}\text{N}$	$^{12}\text{C} + ^{16}\text{O}$	$^{28}\text{Si}$
$a^b$	3.58	3.71	3.71	3.96	3.7	3.84	...	...	...	3.26
$\Delta^b$	5.13	1.8	1.8	0	0.25	2.67	...	...	...	3.89
$Y^c$	0.17	0.17	0.17	...	0.15	0.14	0.20	...	...	0.20
$E_c^d$ (MeV)	10	4.5	2.65	2.5	3.9	2.6	12.5	6	16.5	...
$E_{\max}^e$ (MeV)	25.5	25	21	14.2	12.2	10.9	12.5	6	16.5	...
$V^f$ (MeV)	125.3 <sup>f</sup>	47.2 <sup>g</sup>	48 <sup>h</sup>	117 <sup>i</sup>	155 <sup>j</sup>		$7.5 + 0.4 E_{\text{c.m.}}^k$			
$r_0$ (fm)	4.47 <sup>f</sup>	3.75 <sup>g</sup>	3.81 <sup>h</sup>	3.10 <sup>i</sup>	3.16 <sup>j</sup>		$1.35(A_1^{1/3} + A_2^{1/3})^k$			
$a_0$ (fm)	0.54 <sup>f</sup>	0.65 <sup>g</sup>	0.66 <sup>h</sup>	0.86 <sup>i</sup>	0.80 <sup>j</sup>		0.45 <sup>k</sup>			
$W$ (MeV)	30.7 <sup>f</sup>	7.5 <sup>g</sup>	9.6 <sup>h,1</sup>	18.9 <sup>i</sup>	15.0 <sup>j</sup>		$0.4 + 0.125 E_{\text{c.m.}}^k$			
$r_i$ (fm)	4.60 <sup>f</sup>	3.75 <sup>g</sup>	3.81 <sup>h</sup>	4.7 <sup>i</sup>	5.2 <sup>j</sup>		$1.35(A_1^{1/3} + A_2^{1/3})^k$			
$a_i$ (fm)	0.39 <sup>f</sup>	0.70 <sup>g</sup>	0.47 <sup>h</sup>	0.54 <sup>i</sup>	0.6 <sup>j</sup>		0.45 <sup>k</sup>			
$R_{\text{Coul}}$ (fm)	4.47 <sup>f</sup>	3.75 <sup>g</sup>		3.85 <sup>i</sup>	4.1 <sup>j</sup>		$1.35(A_1^{1/3} + A_2^{1/3})^k$			

<sup>a</sup> The notation is that of Facchini and Saetta-Menichella (Ref. 30), who write

$$\text{level density} = \rho(E) [2(2\pi)^{1/2} \sigma^3]^{-1} P_I \sum_I (2I+1) \exp[-I(I+1)/2\sigma^2],$$

where  $\rho(E) \equiv [\sqrt{\pi}/(12a^{1/4})] U^{-5/4} \exp[2(aU)^{1/2}]$ ,  $U = E - \Delta$ , and  $\sigma^2 = 1.44A^{2/3} \text{ at}/\pi^2$  with  $t = [(E - \Delta)/a]^{1/2}$ .

<sup>b</sup> Values of the parameters have been taken from Ref. 30.

<sup>c</sup>  $E_{\text{Yrast}} = YI(I+1)$  = maximum energy for spin  $I$ .

<sup>d</sup> Energy above which discrete levels were unknown and continuum level densities were used.

<sup>e</sup> Maximum energy for which level densities were calculated.

<sup>f</sup> P. P. Singh, R. E. Malmin, M. High, and D. W. Devins, Phys. Rev. Letters **23**, 1124 (1969).

<sup>g</sup> L. Rosen, Helv. Phys. Acta, Exp. Suppl. **12**, 253 (1966).

<sup>h</sup> F. Perey and B. Buck, Nucl. Phys. **32**, 353 (1962).

<sup>i</sup> T. J. Yule and W. Haerberli, Nucl. Phys. **117**, 1 (1968).

<sup>j</sup> W. P. Alford, D. Cline, H. E. Gove, K. H. Purser, and S. Skorka, Nucl. Phys. **130**, 119 (1969).

<sup>k</sup> R. E. Malmin, Ph.D. thesis, Indiana University, 1972 (unpublished).

<sup>1</sup> The imaginary well was of the surface type in this case; all others were volume.

<sup>m</sup> A deeper well with  $W_i = -17.2 + 1.86E_{\text{c.m.}}$ ,  $r_i = 3.90$  fm, and  $a_i = 0.80$  fm gave nearly identical results.

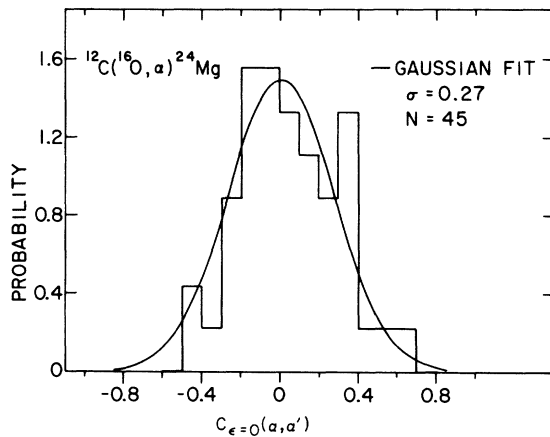


FIG. 7. The measured cross-correlation coefficients plotted as a probability distribution normalized by the factor

$$C_{\epsilon=0}(\alpha, \alpha') = \frac{R_{\epsilon=0}(\alpha, \alpha')}{[R_{\epsilon=0}(\alpha)R_{\epsilon=0}(\alpha')]^{1/2}}.$$

The solid line is a least-squares fit to a Gaussian shape with  $\sigma = 0.27$ . The total number of correlations computed was  $N = 45$ .

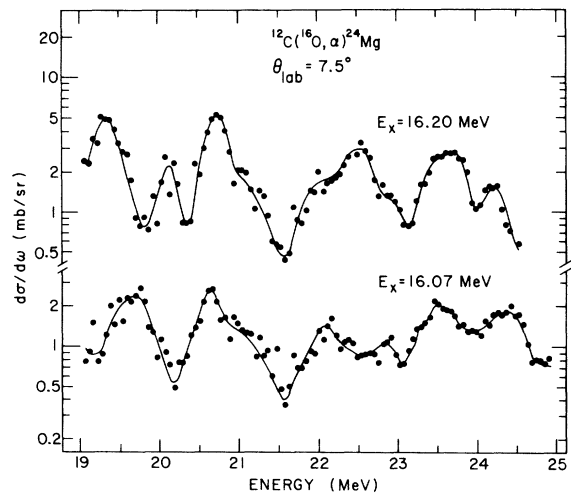


FIG. 8. The excitation functions for the two  $^{24}\text{Mg}$  levels (16.07 and 16.20 MeV) that gave the highest cross correlation (0.62). Even for these two function, the correlations are not striking.

then normalized by the relation

$$C_{\epsilon=0}(\alpha, \alpha'') = \frac{R_{\epsilon=0}(\alpha, \alpha')}{[R_{\epsilon=0}(\alpha)R_{\epsilon=0}(\alpha')]^{1/2}}$$

The resultant cross-correlation coefficients are shown as a probability distribution in Fig. 7. It can be shown<sup>23,24</sup> that the probability distribution for the cross-correlation coefficients between synthetic uncorrelated excitation functions (generated by random numbers) will be a Gaussian symmetric about zero. The figure shows the least-squares fit of a Gaussian (smooth curve) to the measured distribution; it can be seen to describe the data rather well. Even though this is not a rigorous analysis, it shows that the measured cross correlations are compatible with purely statistical fluctuations. That is, we would expect to see substantial deviations from the Gaussian shape if meaningful cross correlations were present. The largest cross correlation was 0.62 for the 16.07- and 16.20-MeV levels. These functions, however, fail to show very striking correlations (Fig. 8).

Furthermore, there does not appear to be any correlation of possible gross structure between the excitation functions as suggested by Gastebois *et al.*<sup>3</sup> Although the excitation functions show evidence of gross structure, this might be expected even for purely random or statistical fluctuations. The correlations reported by Gastebois *et al.*<sup>3</sup> appear to be due to their poor energy resolution and are not substantiated by the present work with high energy resolution. For example, the small fluctuations with coherence widths of 90–150 keV (c.m.) seen in the present work were completely smoothed out in the results of Gastebois *et al.*<sup>3</sup> because their

energy spread was 100–130 keV (c.m.) and their measurements were in steps of 330–500 keV (lab). This is what led them to the conclusion (contradicted in the present work) that statistical fluctuations do not exist.

In summary, although we cannot rule out the presence of a significant direct-reaction component, we conclude that the results of the fluctuation analysis are compatible with a purely statistical compound-nucleus reaction mechanism.

#### V. HAUSER-FESHBACH STATISTICAL MODEL CALCULATIONS

The observed strong and rapid fluctuations in the  $^{12}\text{C}(^{16}\text{O}, \alpha)^{24}\text{Mg}$  reaction are indicative of a compound-nucleus process. The presence of strong prominent states in the spectra, as well as the absence of such states in the  $^{14}\text{N}(^{14}\text{N}, \alpha)^{24}\text{Mg}$  reaction, can be explained by Hauser-Feshbach statistical-model calculations. As discussed previously, such an explanation is in accord with the conclusions reached by Halbert, Durham, and van der Woude<sup>7</sup> from a similar study of the  $^{12}\text{C}(^{16}\text{O}, \alpha)^{24}\text{Mg}$  reaction at lower energies. We also expect this model to explain the presence or absence of prominent states in other heavy-ion reactions such as  $^{12}\text{C}(^{16}\text{O}, p)^{27}\text{Al}$ ,  $^{25}\text{C}(^{18}\text{O}, \alpha)^{26}\text{Mg}$ ,  $^{26}\text{C}(^{12}\text{C}, \alpha)^{22}\text{Ne}$ ,  $^{27}\text{C}(^{16}\text{O}, \alpha)^{26}\text{Mg}$ ,  $^{27}\text{O}(^{16}\text{O}, \alpha)^{28}\text{Si}$ ,  $^{26}\text{Mg}(^{16}\text{O}, \alpha)^{38}\text{Ar}$ ,  $^{27}\text{C}(^{12}\text{C}, \alpha)^{20}\text{Ne}$ ,<sup>8</sup> although we have not explicitly performed calculations for these cases. In view of the present results, it also appears possible that  $(^{14}\text{N}, ^8\text{Li})$ ,  $^{12}\text{C}(^{14}\text{N}, d)^{24}\text{Mg}$ ,<sup>28</sup> or other exotic reactions may proceed via a compound-nucleus process rather than via a direct eight- or twelve-nucleon transfer.

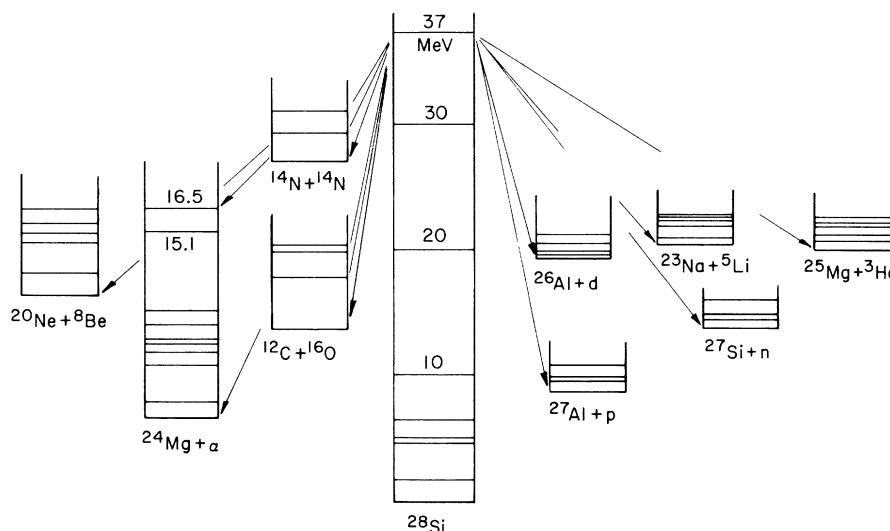


FIG. 9. The compound system  $^{28}\text{Si}$  and the nine most important open channels used in the Hauser-Feshbach calculations. Note that the  $^{14}\text{N}+^{14}\text{N}$  system is at a much higher energy in  $^{28}\text{Si}$  than in the  $^{12}\text{C}+^{16}\text{O}$  system.



It is not clear *a priori*, that the Hauser-Feshbach theory should be applied to heavy-ion reactions, especially in cases involving high angular momentum for which the density of states in the compound nucleus is low. However, the results of Vogt *et al.*<sup>8</sup> and Shaw *et al.*<sup>9</sup> encourage us to believe that such a straightforward application of the statistical model is indeed justified. In retrospect, perhaps the best justification arises from the excellent agreement between the Hauser-Feshbach theory and the available data for the present reaction.

In the Hauser-Feshbach picture, the compound nucleus statistically decays into all available open channels. The larger the number of open channels available, the smaller will be the average flux into each of them. The number of open channels increases rapidly with excitation energy and decreases rapidly with increasing angular momentum in the compound nucleus. For high-spin states in the compound nucleus, there are few open channels (usually involving heavy decay products) which can carry away the angular momentum.

The most important decay channels of the  $^{28}\text{Si}^*$  compound nucleus are shown in Fig. 9. As can be seen, the  $^{14}\text{N}+^{14}\text{N}$  system opens up at a higher energy in  $^{28}\text{Si}^*$  than does the  $^{12}\text{C}+^{16}\text{O}$  system. For the same excitation energy in  $^{28}\text{Si}^*$ , the incident energy must be larger for  $^{12}\text{C}+^{16}\text{O}$ , and therefore the grazing angular momentum will be larger.

The grazing angular momentum, defined as the  $L$  value for which the transmission coefficient falls to  $T_L = \frac{1}{2}$ , is shown in Fig. 10 as a function of excitation energy in various channels. The calculations, performed with the code ABACUS,<sup>29</sup> are for an excitation energy of 38.2 MeV in  $^{28}\text{Si}^*$ , corresponding to an incident energy of 50 MeV for  $^{16}\text{O}$  on  $^{12}\text{C}$ . The optical-model parameters, taken wherever possible from elastic scattering studies, are listed in Table II.

The Hauser-Feshbach denominator  $G(J)$ , defined as the sum of the transmission coefficients for all open channels in the compound nucleus, is plotted in Fig. 11 as a function of the total angular momentum  $J$  for an excitation energy of 38.2 MeV in  $^{28}\text{Si}^*$ .

TABLE III. Calculated peak-to-background ratios for high-spin  $^{24}\text{Mg}$  states populated by the  $^{12}\text{C}(^{16}\text{O}, \alpha)$  and  $^{14}\text{N}(^{14}\text{N}, \alpha)$  reactions at an excitation energy of 38.2 MeV in the compound nucleus  $^{28}\text{Si}$ . A Gaussian-peak shape with a width of 50 keV (FWHM) was assumed.

$J$	$^{12}\text{C}(^{16}\text{O}, \alpha)^{24}\text{Mg}$	$^{14}\text{N}(^{14}\text{N}, \alpha)^{24}\text{Mg}$
6	0.6	0.07
7	1.4	0.08
8	3.1	0.08
9	5.8	0.08
10	10.8	0.08

The number of open channels was determined by summing over all known discrete levels and by using level-density relations for the continuum, as discussed in detail below.

As shown in Fig. 10, the grazing angular momentum in the  $^{12}\text{C}+^{16}\text{O}$  incident channel is  $L_{1/2} = 16\hbar$  at 38.2 MeV in  $^{28}\text{Si}^*$ , whereas that in the  $^{14}\text{N}+^{14}\text{N}$  channel is  $L_{1/2} = 7\hbar$  ( $J=5-9$  in  $^{28}\text{Si}^*$ ). If we now consider the total number of open channels available, as shown by  $G(J)$  in Fig. 11, the  $^{12}\text{C}+^{16}\text{O}$  channel at  $J=16$  has  $G(J) < 10$ , whereas the  $^{14}\text{N}+^{14}\text{N}$  channel at  $J=5-9$  has  $G(J) > 10^4$ . Hence, the largest angular momentum brought into the compound system  $^{28}\text{Si}^*$  by the  $^{12}\text{C}+^{16}\text{O}$  channel can be carried away only through a relatively small number of channels, primarily high-spin states at high excitation in  $^{24}\text{Mg}$ , whereas these high-spin states must compete with a large number of open channels in the  $^{14}\text{N}+^{14}\text{N}$  case. Furthermore, the transitions to the high-spin states in the  $^{12}\text{C}(^{16}\text{O}, \alpha)^{24}\text{Mg}$  reaction will be enhanced in the spectra relative to those low-spin states, since the latter states must compete with a large number of open channels.

The total angular integrated c.m. cross sections were calculated explicitly by use of the Hauser-Feshbach formula

$$\sigma_{\alpha, \alpha'} = \pi \lambda^2 \alpha \sum_J \frac{(2J+1)}{(2I+1)(2i+1)} \frac{\sum_{S I} T_{\alpha S I}^J \sum_{S' I'} T_{\alpha' S' I'}^J}{\sum_{\alpha'' S'' I''} T_{\alpha'' S'' I''}^J},$$

where unprimed quantities refer to the incident channel, primed to the exit channel, and double primed to all possible channels. Each channel  $\alpha$  has channel spin  $S(\vec{S} = \vec{I} + \vec{i})$ , orbital angular momentum  $L$ , and total angular momentum  $J$ ; and  $i$  and  $I$  are

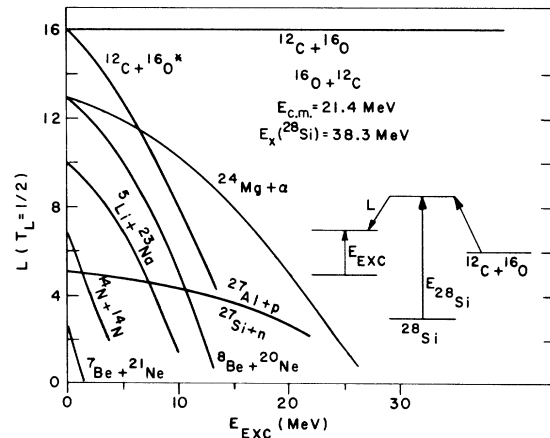


FIG. 10. The grazing angular momentum, defined as the  $L$  value for which the optical-model transmission coefficient is  $\frac{1}{2}$ , for the main reaction channels at an incident energy of 50 MeV. The incident angular momentum in the  $^{12}\text{C}+^{16}\text{O}$  system is  $16\hbar$ .

the intrinsic spins of the incident and target nuclei, respectively. The quantities  $T_{\alpha SI}^J$  are the optical-model transmission coefficients. The denominator is summed over discrete known levels and continuum levels computed by level-density equations.<sup>30</sup> Since identical particles collide in the  $^{14}\text{N} + ^{14}\text{N}$  reaction, its cross section must be multiplied by 2 to take account of restrictions on the possible  $L$  values that can couple with the channel spin (0, 1, or 2). In the calculations, it was assumed that all of the absorption implied by the transmission coefficients was due to compound-nucleus processes. If the direct-reaction components were subtracted, the transmission coefficients (especially for surface partial waves) would be reduced and the cross sections would thus be smaller. The resultant cross sections are thus upper limits for the compound-nucleus contributions.

In order to simplify the calculations of the denominator, the reflection coefficients  $\eta_L(T_L = 1 - |\eta_L|^2)$  were calculated at a number of selected energies and fitted as a function of  $L$  at each energy by a three-parameter Fermi function

$$\eta_L(E) = A_0(E) + [1 - A_0(E)] \times \{1 + \exp[(L_0(E) - L)/\Delta_L(E)]\}^{-1}.$$

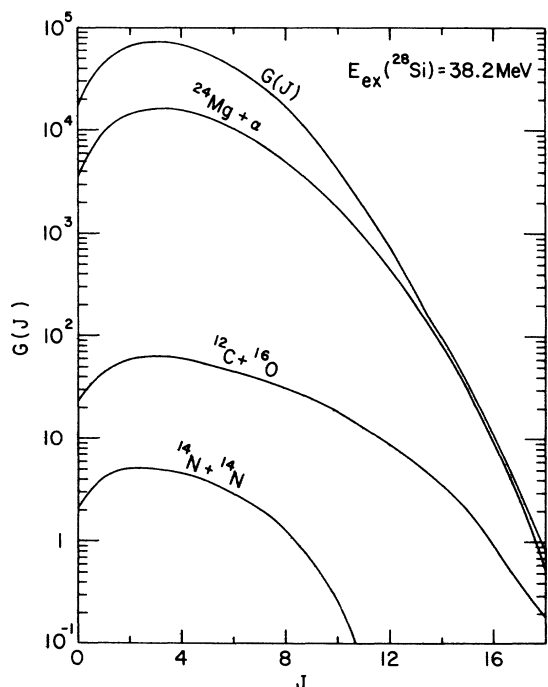


FIG. 11. The Hauser-Feshbach denominator  $G(J)$ , which is equal to the "number of open channels," for the decay of the compound nucleus  $^{28}\text{Si}$  at 38.2 MeV into different spins  $J$ . The total contributions from the  $^{12}\text{C} + ^{16}\text{O}$ ,  $^{14}\text{N} + ^{14}\text{N}$ , and  $^{24}\text{Mg} + \alpha$  channels are also shown. Only decays from natural-parity states in  $^{28}\text{Si}^*$  were included.

The three parameters,  $A_0(E)$ ,  $L_0(E)$ , and  $\Delta_L(E)$  were then fitted to a quadratic function of the energy  $E$ . The procedure was found to be accurate within 10% for all important channels. Exact values of the transmission coefficients were used to calculate the numerator of the Hauser-Feshbach cross section, as well as the most important term in the denominator, the  $^{12}\text{C} + ^{16}\text{O}$  channel. The denominator was explicitly calculated from the relation

$$G(J) = \sum_{\alpha'' SI} \left( \sum_{E_x=0}^{E_c} T_i^J(\alpha'') + \int_{E_c}^{E_{\max}} \rho(E, I) T_i(\alpha'') \right),$$

where the sum from  $E_x = 0$  to  $E_c$  is for known discrete levels and the integral from  $E_c$  to  $E_{\max}$  is for continuum states calculated from the level density  $\rho(E, I)$ . At a given excitation energy in the residual nucleus, the state of maximum allowed angular momentum (yrast level) was determined from  $E_Y(I) = YI(I+1)$ . The parameters  $E_c$ ,  $E_{\max}$ , and  $Y$ , and the level-density equations used are given in Table II. For large  $J$ , the denominator is dominated by the  $^{12}\text{C} + ^{16}\text{O}$  and  $^{24}\text{Mg} + \alpha$  channels, the latter of which is sensitive to the level-density parameters used. However, the qualitative shape of the denominator  $G(J)$  is not affected by these

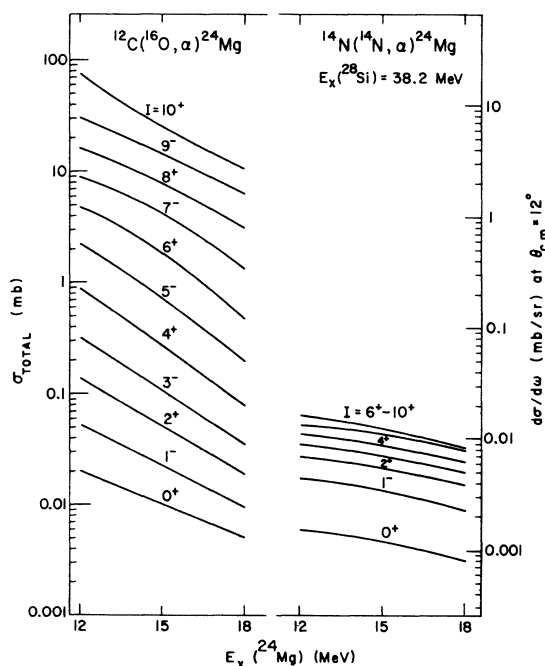


FIG. 12. Total Hauser-Feshbach cross sections for the population of natural-parity states in  $^{24}\text{Mg}$  at  $E_x = 12$ –18 MeV in  $^{24}\text{Mg}$  for an incident energy of 50 MeV ( $E_{\text{c.m.}} = 21.4$  MeV). The right-hand ordinate represents the differential cross section at an angle of  $7.5^\circ$  (lab) ( $\theta_{\text{c.m.}} = 12^\circ$ ) on the assumption of a  $1/\sin\theta$  angular distribution.

uncertainties. The contributions to  $G(J)$  from several important channels are also shown in Fig. 11.

Figure 12 shows the resultant cross sections to various  $I^\pi$  states at 12–18 MeV excitation in  $^{24}\text{Mg}$  formed in the  $(^{16}\text{O}, \alpha)$  reaction at  $E(^{16}\text{O}) = 50$  MeV. The left-hand ordinate is the total cross section and the right-hand ordinate is the differential cross section at  $\theta_{\text{c.m.}} = 12^\circ$  as calculated on the assumption that the angular distribution has a  $1/\sin\theta$  shape. States with  $I_f = 6-10$  are very strongly populated relative to states of lower spin in the  $^{12}\text{C} + ^{16}\text{O}$  reaction, in marked contrast to the  $^{14}\text{N} + ^{14}\text{N}$  results.

Figure 13 shows the partial cross sections for the transition from a state of each  $J$  in  $^{28}\text{Si}$  to states with spins  $I = 0^+, 4^+,$  and  $8^+$  in  $^{24}\text{Mg}$  for both reactions. Clearly, high-spin states in  $^{24}\text{Mg}$  are fed strongly by states of high angular momentum  $J$  in  $^{28}\text{Si}$ , for which there are few open channels. States of lower  $I$  in  $^{24}\text{Mg}$  are seen to be much weaker, since they are fed by lower  $J$  values. For  $^{14}\text{N} + ^{14}\text{N}$  induced reactions, the incident angular momentum is much lower and the states in  $^{24}\text{Mg}$  are fed by a larger range of low  $J$  values

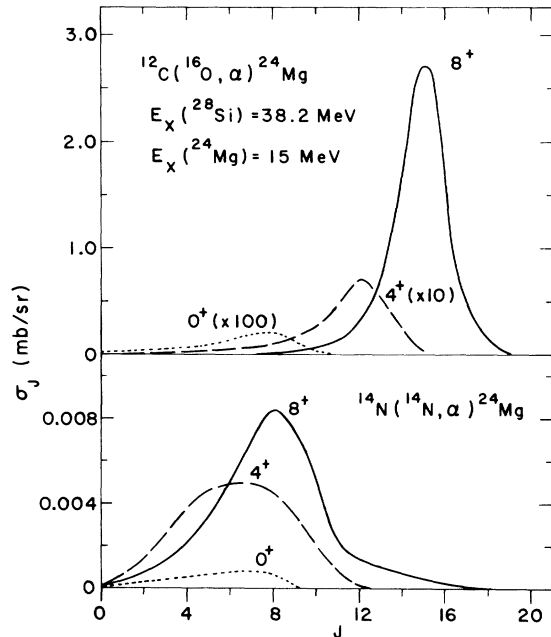


FIG. 13. Partial Hauser-Feshbach cross sections for  $^{12}\text{C}(^{16}\text{O}, \alpha)^{24}\text{Mg}$  and  $^{14}\text{N}(^{14}\text{N}, \alpha)^{24}\text{Mg}$  reactions, plotted as a function of total angular momentum  $J$ . The calculations were for decays from the 38.2-MeV level in the compound nucleus  $^{28}\text{Si}$  to  $^{24}\text{Mg}$  levels having the indicated  $I^\pi$  and energies near  $E_x = 15$  MeV. Note that the  $4^+$  and  $0^+$  cross sections are multiplied by factors of 10 and 100, respectively, for the  $^{12}\text{C}(^{16}\text{O}, \alpha)^{24}\text{Mg}$  reaction, whereas the cross sections for the  $^{14}\text{N}(^{14}\text{N}, \alpha)^{24}\text{Mg}$  reaction require no such scale factors.

than in  $^{12}\text{C} + ^{16}\text{O}$  reactions, as seen in Fig. 13. The marked difference between the  $^{12}\text{C} + ^{16}\text{O}$  spectra and the  $^{14}\text{N} + ^{14}\text{N}$  spectra can be easily understood from Figs. 12 and 13.

In order to show that the high-spin states in  $^{24}\text{Mg}$  should be prominent in the  $^{12}\text{C} + ^{16}\text{O}$  case and not in the  $^{14}\text{N} + ^{14}\text{N}$  case, peak-to-background ratios were calculated (Table III) on the assumption that all of the prominent levels have  $I \geq 6$  and that the background consists of all levels with  $I \leq 5$ . A Gaussian peak shape with a width of 50 keV (FWHM) was used. Clearly, the calculations predict that the  $^{12}\text{C} + ^{16}\text{O}$  spectra should have prominent peaks for high-spin states, whereas the  $^{14}\text{N} + ^{14}\text{N}$  spectra will be smooth.

#### VI. COMPARISON OF CALCULATIONS WITH EXPERIMENTAL DATA

The computed Hauser-Feshbach cross sections have been compared both with the present data and with other studies. Table I shows a comparison between the measured cross sections for the  $^{12}\text{C}(^{16}\text{O}, \alpha)^{24}\text{Mg}$  reaction, averaged over the energy interval  $E_{\text{c.m.}} = 19-25$  MeV, and the computed Hauser-Feshbach cross sections, similarly averaged and estimated at  $\theta_{\text{c.m.}} = 12^\circ$  on the assumption of a  $1/\sin\theta$  angular distribution. Since only three

TABLE IV. Comparison of theoretical Hauser-Feshbach cross sections  $\sigma_T^{\text{H.F.}}$  with experimental data  $\sigma_T^{\text{exp}}$  for the  $^{12}\text{C}(^{16}\text{O}, \alpha)^{24}\text{Mg}$  reaction.

$E_x$ (MeV)	$J^\pi$	$\sigma_T^{\text{exp}}$ (mb)	$\sigma_T^{\text{H.F.}}$ (mb)
0	$0^+$	$2.87 \pm 0.34^a$	$2.6^b$
1.37	$2^+$	$6.42 \pm 0.50^a$	$6.4^b$
4.12	$4^+$	$13.85 \pm 0.8^a$	$8.8$
4.23	$2^+$		$4.7$
5.22	$3^+$	$6.21 \pm 0.46^a$	$4.0^b$
6.00	$4^+$	$9.39 \pm 0.28^a$	$7.2$
6.44	$0^+$		$0.8$
5.22	$3^+$	$7.9^c$	$5.0^d$
6.00	$4^+$	$9.8^c$	$8.0^d$
6.44	$0^+$	$1.7^c$	$0.9^d$
7.35	$2^+$	$3.0^c$	$2.7^d$
8.12	$6^+$	$14.0^c$	$11.0^d$
9.28	...	$17.5^c$	$6^+ 8.0^d$ $7^- 10.0^d$ $8^+ 22.0^d$

<sup>a</sup> Measurement by Halbert, Durham, and van der Woude (Ref. 7) at  $E_{\text{c.m.}} = 12.5-14$  MeV.

<sup>b</sup> Calculated for  $E_{\text{c.m.}} = 12.85$  MeV.

<sup>c</sup> Measurement by Middleton *et al.* (Ref. 6) at  $E_{\text{c.m.}} = 13.5-14.5$  MeV. This value of  $\sigma_T$  was estimated by integrating energy-averaged angular distributions with unknown error.

<sup>d</sup> Calculated for  $E_{\text{c.m.}} = 14.2$  MeV.

levels have known  $J^\pi$  values, this comparison is unfortunately very limited. Nevertheless, the values are in reasonable agreement, generally within a factor of 2.

The computed cross sections have also been compared with the total  $\alpha$  yields, as shown in Fig. 5. The Hauser-Feshbach cross sections were computed for the excitation range  $E_x = 13.5$ – $17.5$  MeV covered by the counter. The total cross section is fitted very well, especially at lower energies.

The sum of the cross sections for reactions to the 10 most prominent levels, for which we assume  $I \geq 6$ , is lower than the calculated curve, while the background (assumed to arise from levels with  $I \leq 5$ ) is higher than the computed curve. This might be explained by assuming that some of the less prominent levels not included in the sum have  $I \geq 6$ , since the total cross section is fitted quite well. Generally, the calculated cross sections fit the data quite well; however, a more detailed comparison must await more precise determinations of  $I^\pi$ .

The theoretical calculations have also been compared (Table IV) with the total energy-averaged and angular integrated cross sections of Halbert, Durham, and van der Woude<sup>7</sup> for the first few excited states in  $^{24}\text{Mg}$ . The measured cross sections agree very well with the calculations. Furthermore, Halbert, Durham, and van der Woude have shown that the reaction mechanism for these states is well described by the compound-nucleus picture.

Furthermore, we have compared (Table IV) the calculations with the energy-averaged angular distributions of Middleton *et al.*<sup>6</sup> for excitation energies  $E_x = 5.22$ – $9.28$  MeV in  $^{24}\text{Mg}$  at incident energies  $E_{c.m.} = 13.5$ – $14.5$  MeV. As previously noted, these angular distributions appear to be well described by the function  $1/\sin\theta$  and the total cross sections agree rather well with calculations.

The computed cross sections for the  $^{14}\text{N}(^{14}\text{N}, \alpha)^{24}\text{Mg}$  reaction are compared directly with the measured values of Middleton, Garrett, and Fortune<sup>31</sup> in Table V. In general, the computed values appear to be about a factor of 3 too high, depending on the optical parameters used. Both the potential given in Table II (based on  $^{12}\text{C} + ^{16}\text{O}$  scattering)<sup>10</sup> and a potential derived by Gobbi *et al.*<sup>11</sup> for  $^{14}\text{N} + ^{14}\text{N}$  scattering were tried. The two results were similar. There are several possible reasons for the discrepancy between the calculations and the data. First, the  $^{14}\text{N} + ^{14}\text{N}$  optical-model parameters are not well established. This might be very important since the computed transmission coefficients appear to be changing rapidly in this energy region. Secondly, the cross sections, measured at only one angle and energy, are subject to local fluctuations which might produce large errors (e.g., the

present excitation functions in Figs. 3 and 4 show order-of-magnitude fluctuations).

#### VII. CALCULATION OF COHERENCE WIDTHS AND FIT TO HAUSER-FESHBACH DENOMINATOR

The coherence widths calculated with the Hauser-Feshbach theory may be compared with the average coherence widths  $\Gamma = \langle \Gamma_J \rangle$  derived from the fluctuation analysis. The latter values of  $\Gamma$  are given by the weighted sum

$$\frac{1}{\Gamma} = \left[ \frac{\sum_J (P_J / \Gamma_J)}{\sum_J P_J} \right],$$

where  $P_J$  is a weighting function and  $\sum_J$  is over the partial widths  $\Gamma_J$  in  $^{28}\text{Si}$ . The latter are obtained from the relationship<sup>20</sup>

$$\Gamma_J = \frac{G(J)}{[2\pi\rho(E_c)/2\sigma^2](2J+1)\exp[-J(J+1)/2\sigma^2]},$$

where  $G(J)$  is the Hauser-Feshbach denominator,  $\rho(E_c)$  is the level density, and  $2\sigma^2$  is the spin-cutoff

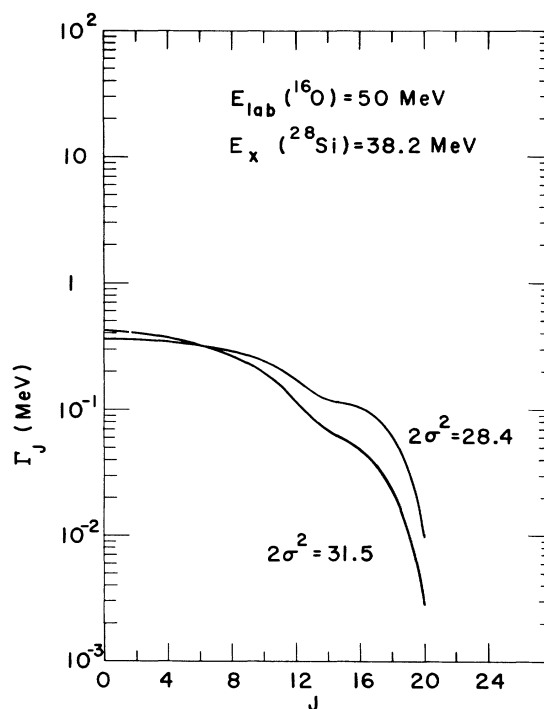


FIG. 14. Partial widths  $\Gamma_J$  as a function of total angular momentum  $J$  at 38.2 MeV in the compound nucleus  $^{28}\text{Si}$  for two different values of  $2\sigma^2$ . The top curve ( $2\sigma^2 = 28.4$ ) was calculated with the level-density parameters (Ref. 30) and corresponds to a rigid-body moment of inertia model with radius  $r = 1.33$  fm. The bottom curve was calculated with  $2\sigma^2 = 31.5$  ( $r = 1.40$  fm). Note that  $\Gamma_J$  is not independent of  $J$  as was assumed in Sec. VII.

parameter in  $^{28}\text{Si}$ . Such calculations appear to be quite sensitive to the value chosen for  $2\sigma^2$ , as shown in Fig. 14, but the relative values of the coherence widths for different values of  $I$  in  $^{24}\text{Mg}$  are independent of it.

If  $P_f$  is taken as the compound-nucleus formation cross section, then  $\Gamma = 140$  keV at  $E_{\text{lab}} = 50$  MeV. However, a physically more reasonable weighting function is the actual Hauser-Feshbach cross section for the decay of a  $^{28}\text{Si}^*$  state with total angular momentum  $J$  to a state with given  $I^\pi$  and excitation energy in  $^{24}\text{Mg}^*$  (Fig. 13). This procedure appears to predict the dependence of  $\Gamma$  on the  $I^\pi$  value and the excitation energy in  $^{24}\text{Mg}$ , as shown in Fig. 15. The data points are the coherence widths measured in the fluctuation analysis on the assumption that the finite size of the data sample contributes a 20% error. The spin-cutoff parameter was arbitrarily chosen at  $2\sigma^2 = 30$  to best fit the magnitude of the data. The shapes of the calculated curves do not depend on the value of  $2\sigma^2$  chosen. This corresponds to a rigid-body moment-of-inertia calculation with a radius of 1.37 fm. This value is not unreasonable, since a similar value was obtained by Shaw *et al.*<sup>9</sup> for the  $^{16}\text{O}(^{16}\text{O}, \alpha)^{28}\text{Si}$  reaction at lower energies in  $^{28}\text{Si}$ . Although the absolute values calculated for the coherence widths should probably not be taken seriously, the relative dependences on  $I^\pi$  and excitation energy in  $^{24}\text{Mg}$  agree rather well with the data. This demonstrates that the observed coherence widths are compatible with the statistical model.

Both the coherence widths derived in the present work and the computed values agree rather well

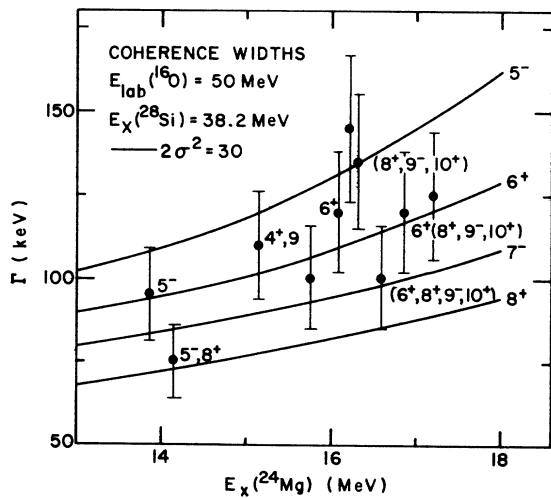


FIG. 15. Comparison between the coherence widths derived from the fluctuation analysis (points) and those calculated from Hauser-Feshbach theory (curves). Calculations were performed with  $2\sigma^2 = 30$  at  $E_{\text{lab}} = 50$  MeV.

with other studies. Halbert, Durham, and van der Woude<sup>7</sup> found an average coherence width  $\Gamma = 118 \pm 17$  keV for the  $^{12}\text{C}(^{16}\text{O}, \alpha)^{24}\text{Mg}$  reaction at lower incident energies and excitation in  $^{24}\text{Mg}$ . Similar studies by Vogt *et al.*<sup>8</sup> for the  $^{12}\text{C}(^{12}\text{C}, \alpha)^{20}\text{Ne}$  reaction and by Shaw *et al.*<sup>9</sup> for the  $^{16}\text{O}(^{16}\text{O}, \alpha)^{28}\text{Si}$  reaction also have found reasonable agreement between experimentally derived coherence widths and those computed from the Hauser-Feshbach statistical model. However, the widths found in the present study may not be compatible with the results of

TABLE V. Comparison between calculated Hauser-Feshbach cross sections and the measured cross sections for the  $^{14}\text{N}(^{14}\text{N}, \alpha)^{24}\text{Mg}$  reaction.

$E_x$ (MeV)	$(d\sigma/d\omega)_{\text{exp}}^a$ ( $\mu\text{b}/\text{sr}$ )	$J^\pi$	$(d\sigma/d\omega)_{\text{H.F.}}^b$ ( $\mu\text{b}/\text{sr}$ )
0.0	<1	0 <sup>+</sup>	3.3
1.37	6	2 <sup>+</sup>	13
4.12	6	4 <sup>+</sup>	20
4.23	4	2 <sup>+</sup>	12
5.22	2	3 <sup>+</sup>	12
6.00	5	4 <sup>+</sup>	20
6.44	1	0 <sup>+</sup>	3.0
7.35	4	2 <sup>+</sup>	12
7.56	2	1 <sup>-</sup>	7
7.62	3	3 <sup>-</sup>	15
7.75	5	1 <sup>+</sup>	3.0
7.81	3	(5 <sup>+</sup> )	19
8.12	6	6 <sup>+</sup>	21
8.36	8	3 <sup>-</sup>	15
8.44	8	{ 1 <sup>-</sup> (4 <sup>+</sup> )	{ 7 18
8.65	~1	2 <sup>+</sup>	12
8.86	3	2 <sup>-</sup>	7
9.00	5	2 <sup>+</sup>	11
9.15	3	1 <sup>-</sup>	7
9.28	12	{ 2 <sup>+</sup> 3 <sup>-</sup> 4 <sup>+</sup>	{ 11 15 18
9.46	6	{ 2 <sup>+</sup> 3 <sup>-</sup> 4 <sup>+</sup>	{ 11 15 18
9.52	5	{ 4 <sup>+</sup> 6 <sup>+</sup>	{ 18 21
9.83	5	(1 <sup>+</sup> )	2.0
9.96	≤2	1 <sup>+</sup>	2.0
10.02	}	{ 2 <sup>+</sup>	...
10.06			
10.16	4	...	...
10.35	6	...	...
10.58	17	2 <sup>+</sup>	11
10.58	10	...	...
10.66	4	0 <sup>+</sup>	3

<sup>a</sup> Obtained at  $E_{\text{c.m.}} = 10.1$  MeV,  $\theta_{\text{lab}} = 7.5^\circ$  by Middleton, Garrett, and Fortune (Ref. 31). The estimated error is  $\pm 30\%$ .

<sup>b</sup> Present work. The values were calculated on the assumption of a  $1/\sin\theta$  angular distribution.

TABLE VI. Calculated least-squares fit to the approximate form of Eberhard *et al.* (Ref. 33) for the Hauser-Feshbach denominator

$$G(J) = (2\pi\Gamma_0/D_0)(2J+1) \exp[-J(J+1)/2\sigma^2].$$

$E_{\text{c.m.}}$ (MeV)	$J_{\text{max}}^a$	$2\sigma^2$	$2\pi\Gamma_0/D_0$
17.2	$\leq 20$	20.6	3431
	$\leq 12$	22.1	3269
21.4	$\leq 20$	23.7	18 936
	$\leq 12$	25.6	17 149
25.7	$\leq 20$	26.5	93 097
	$\leq 12$	28.6	79 480

<sup>a</sup> Highest value of  $J$  used in the least-squares fit.

other studies, such as  $^{24}\text{Mg}(\alpha, \alpha)^{24}\text{Mg}$ ,<sup>23</sup> or  $^{27}\text{Al}(p, \gamma)^{28}\text{Si}$ .<sup>32</sup>

For convenient comparison with other studies, the Hauser-Feshbach denominator has been fitted to the approximate form of Eberhard *et al.*<sup>33</sup> on the assumption that  $\Gamma_J \approx \Gamma_0$ , independent of  $J$ . This expression is

$$G(J) = 2\pi(\Gamma_0/D_0)(2J+1) \exp[-J(J+1)/2\sigma^2],$$

$$D_0 \approx 2\sigma^2/\rho(E_c),$$

where  $\Gamma_0/D_0$  is the ratio of coherence width to level spacing for spin-zero levels in the compound nucleus  $^{28}\text{Si}$  and  $\sigma^2$  is the spin-cutoff parameter. It was found that the entire  $G(J)$  function could not be well fitted with this simple expression. Consequently, the denominators were also fitted with a calculation in which high  $J$  values were excluded.

The computed values of  $\Gamma_0/D_0$  and  $2\sigma^2$  are listed in Table VI. It should be pointed out that the use of such a formula in our case would not agree very well with the actual calculated cross sections because the errors on  $G(J)$  for high  $J$  values are relatively large. Furthermore,  $\Gamma_J$  is clearly not independent of  $J$ , as shown in Fig. 14.

### VIII. CONCLUSIONS

In conclusion, we find that all of the available data are consistent with the compound-nucleus statistical model. Although we cannot rule out the presence of a direct-reaction component, there does not appear to be any compelling evidence that such a process is present. Contrary to the conclusions of previous studies,<sup>2,3,6</sup> there is no indication of a direct excitation of "quartet states" in  $^{28}\text{Si}$ . These states should exhibit much larger yields than are predicted by a statistical compound-nucleus process and should produce definite gross structure or cross correlations in the excitation functions, but no such effects are evident in the present work. The success of the Hauser-Feshbach statistical model in describing the present data, as well as in other studies, would lead us to suggest that other similar heavy-ion reactions also proceed predominantly by a compound-nucleus reaction mechanism.

### ACKNOWLEDGMENT

The authors would like to thank J. Kulaga for his help with the data reduction, and W. R. Gibbs and A. Richter for their calculations of  $N_{\text{eff}}$  for the present reaction.

†Work performed under the auspices of the U. S. Atomic Energy Commission.

<sup>1</sup>R. Middleton, J. D. Garrett, and H. T. Fortune, *Bull. Am. Phys. Soc.* **16**, 37 (1971).

<sup>2</sup>A. Gobbi, P. R. Maurenzig, L. Chua, R. Hadsell, P. D. Parker, M. W. Sachs, D. Shapiro, R. Stokstad, R. Wieland, and D. A. Bromley, *Phys. Rev. Letters* **26**, 396 (1971).

<sup>3</sup>J. Gastebois, R. Ballini, P. Charles, B. Fernandez, and J. Fouan, *Lettere Nuovo Cimento* **2**, 90 (1971); J. Gastebois, *J. Phys. (Paris) Suppl.* **32**, C6-57 (1971).

<sup>4</sup>R. Middleton, J. D. Garrett, and H. T. Fortune, *Phys. Rev. Letters* **24**, 1436 (1970).

<sup>5</sup>D. P. Balamuth, J. E. Holden, J. W. Noe, and R. W. Zurmuhle, *Phys. Rev. Letters* **26**, 1271 (1971).

<sup>6</sup>R. Middleton, J. D. Garrett, H. T. Fortune, and R. R. Betts, *J. Phys. (Paris) Suppl.* **32**, C6-39 (1971); *Phys. Rev. Letters* **27**, 950 (1971); and private communication.

<sup>7</sup>M. L. Halbert, F. E. Durham, and A. van der Woude, *Phys. Rev.* **162**, 899, 919 (1967).

<sup>8</sup>E. W. Vogt, D. McPherson, J. Kuehner, and E. Alm-

qvist, *Phys. Rev.* **136**, 99 (1964).

<sup>9</sup>R. W. Shaw, J. C. Norman, R. Vandenbosch, and C. J. Bishop, *Phys. Rev.* **184**, 1040 (1969).

<sup>10</sup>R. E. Malmin, Ph.D. thesis, Indiana University, 1972 (unpublished).

<sup>11</sup>A. Gobbi, Argonne National Laboratory Topical Report No. ANL-7837, 1971 (unpublished), p. 63.

<sup>12</sup>J. C. Stoltzfus, K. Katori, L. R. Greenwood, and T. H. Braid, *Bull. Am. Phys. Soc.* **16**, 581 (1971).

<sup>13</sup>L. R. Greenwood, T. H. Braid, K. Katori, J. C. Stoltzfus, and R. H. Siemssen, *J. Phys. (Paris) Suppl.* **32**, C6-199 (1971).

<sup>14</sup>R. E. Malmin, K. Katori, L. R. Greenwood, T. H. Braid, and R. H. Siemssen, *J. Phys. (Paris) Suppl.* **32**, C6-223 (1971).

<sup>15</sup>R. G. Stokstad, A. Gobbi, P. R. Maurenzig, and R. Wieland, *Bull. Am. Phys. Soc.* **15**, 1677 (1970).

<sup>16</sup>E. R. Cosman, A. Sperduto, T. Cormier, T. Chin, H. Wegner, M. Levine, and D. Schwalm, *Bull. Am. Phys. Soc.* **17**, 489 (1972).

<sup>17</sup>C. J. Borkowski and M. K. Kopp, *IEEE Trans. Nucl.*

Sci. NS-17, 340 (1970).

<sup>18</sup>J. R. Comfort, Argonne Physics Division Informal Report PHY-1970B, 1970 (unpublished).

<sup>19</sup>T. D. Thomas, *Ann. Rev. Nucl. Sci.* **18**, 343 (1968).

<sup>20</sup>T. Ericson, *Ann. Phys. (N.Y.)* **23**, 390 (1963).

<sup>21</sup>R. O. Stephen, Clarendon Laboratory Report, University of Oxford, 1963 (unpublished).

<sup>22</sup>W. R. Gibbs, private communication; A. Richter, private communication.

<sup>23</sup>J. D. A. Roeders, Ph.D. thesis, University of Groningen, 1971 (unpublished).

<sup>24</sup>E. Almqvist, J. A. Kuehner, D. McPherson, and E. W. Vogt, *Phys. Rev.* **136**, B84 (1964).

<sup>25</sup>E. R. Cosman, A. Sperduto, W. H. Moore, T. N. Chin, and T. M. Cormier, *Phys. Rev. Letters* **27**, 1074 (1971).

<sup>26</sup>M. J. Levine, private communication.

<sup>27</sup>M. Conjeaud, S. Harar, E. Da Silveira, and C. Volant, Centre d'Etudes Nucléaires, Saclay, Report No. CEA-N-1522, 1971 (unpublished), p. 13.

<sup>28</sup>H. V. Klapdor, N. Marquardt, and H. Reiss, *J. Phys. (Paris) Suppl.* **32**, C6-217 (1971).

<sup>29</sup>E. H. Auerbach, unpublished.

<sup>30</sup>U. Facchini and E. Saetta-Menichella, *Energia Nucl.* **15**, 54 (1968).

<sup>31</sup>R. Middleton, J. D. Garrett, and H. T. Fortune, *Phys. Rev. C* **4**, 1987 (1971).

<sup>32</sup>P. P. Singh, R. E. Segel, L. Meyer-Schützmeister, S. C. Hanna, and R. G. Allas, *Nucl. Phys.* **65**, 577 (1965).

<sup>33</sup>K. A. Eberhard, P. von Brentano, M. Böhning, and R. O. Stephen, *Nucl. Phys.* **A125**, 673 (1969).

PHYSICAL REVIEW C

VOLUME 6, NUMBER 6

DECEMBER 1972

## <sup>50</sup>Ti(*p, p'*γ) Angular-Correlation Study at Isobaric Analog Resonances\*

J. F. Morgan, N. L. Gearhart, H. J. Hausman, J. J. Kent, †

G. A. Norton, and J. W. D. Sinclair

*Department of Physics, The Ohio State University, Columbus, Ohio 43210*

(Received 19 July 1972)

Angular correlations have been measured near several isobaric analog resonances observed in the <sup>50</sup>Ti(*p, p'*γ) reaction populating the <sup>50</sup>Ti 2<sup>+</sup> state at 1.555 MeV. In this manner the limitations on the *J* values of parent states in <sup>51</sup>Ti were obtained. Combining the present results with the *l* values previously obtained from <sup>50</sup>Ti(*d, p*) gives the following *J<sup>π</sup>* values for the indicated parent states: 2.136 MeV,  $\frac{3}{2}^-$  or  $\frac{1}{2}^-$ ; 2.189 MeV,  $\frac{3}{2}^-$ ; 2.896 MeV,  $\frac{1}{2}^-$ ; 2.92 MeV,  $\geq \frac{3}{2}^-$ ; and 3.164 MeV,  $\frac{3}{2}^-$ . The wave function of the 2.189-MeV state of <sup>51</sup>Ti is shown to have configurations other than the previously known *p*<sub>3/2</sub> neutron coupled to <sup>50</sup>Ti 2<sup>+</sup> component.

### I. INTRODUCTION

The analogs of the excited states of <sup>51</sup>Ti were first studied by Cosman, Slater, and Spencer<sup>1</sup> in the inelastic scattering of protons from <sup>50</sup>Ti. Below a bombarding energy of 5 MeV the excitation function of protons inelastically scattered from the 2<sup>+</sup> first excited state (1.55 MeV) displayed three prominent resonances at lab energies of 3.620, 4.315, and 4.575 MeV which were identified as the analogs of the three *p*-wave states observed in <sup>50</sup>Ti(*d, p*) at 2.189, 2.896, and 3.164 MeV. Superimposed on this gross structure there were fine-structure fragments with width and spacings of approximately 15 keV. The fine structure was attributed to fluctuations in the density of the *T<sub>z</sub>* states in the compound nucleus <sup>51</sup>V which have the same *J<sup>π</sup>* as the analog state.

Later Price<sup>3</sup> studied the lowest of these three resonances by observing the γ rays from the <sup>50</sup>Ti-(*p, p'*γ) and the <sup>50</sup>Ti(*p, γ*) reactions. Using a very thin target (<1 keV) he was able to resolve the 3.62-MeV structure into two distinct resonances

located at lab energies of 3.598 and 3.614 MeV, respectively, each having a total width of approximately 4 keV. From the angular distributions of the γ rays observed at each resonance, Price assigned the 3.598-MeV resonance as the analog of the *f*-wave state in <sup>51</sup>Ti at 2.136 MeV and the 3.614-MeV resonance as the analog of the *p*-wave state at 2.189 MeV. This assignment implies a Coulomb displacement energy of 7770 keV for the *f*-wave state and 7733 keV for the *p*-wave state. Cosman *et al.*<sup>1</sup> found the same resonance energy for the analog of the 2.189-MeV state, but quoted average Coulomb displacement energies of 7702 keV and 7739 keV for the *p*-wave states and *f*-wave states, respectively. This is the same difference in Coulomb displacement energies (37 keV) obtained from the results of Price, but Cosman *et al.* apparently used an erroneous neutron separation energy, *S<sub>n</sub>*, for <sup>51</sup>Ti. We use *S<sub>n</sub>* = 6378.7 keV<sup>4</sup> to obtain the displacement energies from the resonance energies of Price. From a study of <sup>50</sup>Ti-(*p, γ*) at the analog of the <sup>51</sup>Ti *p*<sub>3/2</sub> ground state, Maripuu obtained a Coulomb displacement energy